Using Distributed Wearable Inertial Sensors to Measure and Evaluate the Motions of Children with Cerebral Palsy in Hippotherapy

Sen Qiu[1], Jie Li[1(✉)], Zhelong Wang[1], Hongyu Zhao[1], Bing Liang[2], Jiaxin Wang[1], Ning Yang[1], Xin Shi[1], Ruichen Liu[1], Jinxiao Li[1], and Xiaoyang Li[3]

[1] School of Control Science and Engineering, Dalian University of Technology, Dalian 116024, China
{qiu,wangzl}@dlut.edu.cn,
{1165530693,wangjx19890828,yangn_Y,sx,Lrichard}@mail.dlut.edu.cn,
zhy.lucy@hotmail.com, kindawnli@163.com

[2] Suzhou Industrial Park Boai School & Clinic, Suzhou 215000, China
jsboai@163.com

[3] Dalian Qiyu Ipony Equestrian Club Co., Ltd., Dalian 116024, China
3188812@qq.com

Abstract. Cerebral palsy (CP) is a group of nonprogressive neurodevelopmental conditions occurring in early childhood that causes movement disorders and physical disability. Measuring activity levels and gait patterns is an important aspect of rehabilitation programs for CP. Hippotherapy is a rehabilitation method to improve motor coordination ability of children with CP. However, there is still no practical evidence for the effectiveness of hippotherapy. This paper introduces a method of motor measurement and evaluation for children with CP based on body area sensor network. Our method uses wearable inertial sensors to measure the motor function of children with CP by sensor fusion algorithm, whose accuracy is verified by optical system. In addition, via introducing the control group, the differences of motor coordination ability and gait parameters between CP and healthy children were discussed. Generally speaking, our method can effectively measure the movement posture and gait parameters of children with CP during hippotherapy, which provides a basis for proving the effectiveness of hippotherapy.

Keywords: Body sensor network · Hippotherapy · Gait analysis · Sensor fusion · Rehabilitation therapy

This work was supported by National Natural Science Foundation of China under Grant No. 61873044, No. 61803072 and No. 61903062 Dalian Science and Technology Innovation fund (2018J12SN077, 2019J13SN99), National Defense Pre-Research Foundation under Grant No. 614250607011708, Fundamental Research Funds for the Central Universities (DUT18RC(4)036) and China Postdoctoral Science Foundation No. 2017M621131 and No. 2017M621132.

L. Mucchi et al. (Eds.): BODYNETS 2019, LNICST 297, pp. 332–346, 2019.
https://doi.org/10.1007/978-3-030-34833-5_25

1 Introduction

CP is a group of neurological disorders that occur in early childhood or infancy, and affect muscle coordination, body movement, and balance [1,2]. At present, there are many motion rehabilitation therapies for children with CP, such as hydrotherapy intervention [3], massage therapy [4], surgical intervention [5], etc. Hippotherapy is one kind of the motor rehabilitation therapies for children with CP which grows up in western from the middle of last century. It is a kind of rehabilitation method that uses horse as a therapeutic tool to treat various functional and physical, psychological, cognitive, social and behavioral disorders of neurotic children utilizing the regular motion model of horse and the characteristics of human-horse interaction under the guidance of physical, occupational and speech therapists [6]. It is an important part of the overall rehabilitation training program to achieve the ultimate goal of functional rehabilitation. In hippotherapy, the children does not require learning horseback riding skills, but is based on improving the functional and sensory integration of the nervous system. At present, hippotherapy has been used to treat most neurological diseases, such as autism, cerebral palsy, arthritis, multiple sclerosis, craniocerebral injury, stroke, spinal cord injury, behavioral and mental disorders. For children with CP, after sitting on the horse's back, their muscles naturally relax [7]. As children with CP usually have scissors feet, when sitting on the horse's back, their feet will open naturally. By interacting with the horse, which can improve their perception and muscle coordination.

In previous studies, Lee et al. studied the effect of hippotherapy on the recovery of gait and balance ability of stroke patients [8]. Through statistical analysis of the therapeutic effect of hippotherapy on 30 stroke patients for 8 weeks, the effectiveness of hippotherapy was proved. Lee [9] et al. studied the effects of hippotherapy on brain function and blood-derived neurotrophic factor (BDNF) levels in children with attention deficit hyperactivity disorder (ADHD). By comparing the results of brain magnetic resonance imaging scans of 20 children with ADHD after 32 weeks of hippotherapy and the baseline of blood BDNF levels with the parameters of healthy children, it was proved that hippotherapy had a positive effect on the recovery of brain function in children with ADHD. Park et al. [10]discussed the effect of hippotherapy on gross motor function of children with CP. By analyzing the improvement of gross motor function of 34 children with CP after 8 weeks of hippotherapy, the presented results imply a positive effect of the equestrian therapy to improve motor function of children with CP. Above studies mainly used medical measurement methods to evaluate the effects of hippotherapy on gross motor function and behavioral disorders. Such an evaluation method is generally time-consuming and laborious, requiring higher cost output.

Current medical studies have shown that hippotherapy is effective for many diseases, but due to the inherent difficulties in collecting objective data and the lack of effective evaluation methods, the related research progress of hippotherapy is slow. With the development of micro-electro-mechanical system (MEMS), wireless communication and sensor network technology, wireless body sensor net-

work (BSN) -a kind of wireless sensor network (WSN) [11], which is composed of multiple sensor nodes (each capable of data acquisition, processing and communication) placed on different parts of human body are gradually applied in the fields of medical rehabilitation [12], motion analysis [13] and so on. However, the evaluation of motor rehabilitation of children with CP mainly focuses on the monitoring of their motor coordination ability and joint movement, these are what BAN is good at. Therefore, it is feasible to apply BAN to the evaluation of the curative effect of hippotherapy.

Aiming at the current development of hippotherapy, this paper introduces a method of motor measurement and evaluation for children with CP based on body area sensor network. In our research, the motion data of children with CP during equestrian treatment were measured by arranging inertial sensor nodes on the motor dysfunction area of children with CP. One sensor fusion algorithm is adopted for sensor fusion whose accuracy is verified by optical system. In addition, via introducing the control group, the differences of motor coordination ability and gait parameters between children with CP and healthy children were discussed. The results show that our method can effectively measure the movement posture and gait parameters of children with CP during hippotherapy, which provides a basis for proving the effectiveness of hippotherapy.

2 System Platform and Experimental Description

In this section, the system hardware, participants and protocols of experiment will be introduced.

2.1 Experimental Scenario and Platform

In this research, the motion capture system was used (which is developed by our "LIS" Laboratory) to collect the raw sensor data in training. Our system consists several sensor nodes and one sink node, each sensor node equips with MEMS sensors and a radio frequency module. The motion information collected by the sensor, including acceleration, angular velocity and magnetic field intensity, will be written into the SD card in real time under working condition. The sink node contains a LoRa RF module, which works in 433MHz. The highest sample frequency can up 400 Hz. The MEMS sensors is one kind of industrial high precision inertial sensor-ADIS16448, which is equipped with a 3-axis gyroscope, a 3-axis accelerometer, and a 3-axis magnetometer, Table 1 shows their specifications. Figure 1 shows the hardware setup of the system.

2.2 Participants and Protocols

In our case study, four participants (1 healthy children, male; 3 children with CP, 1 male, 2 females) and one horse were recruited to participate in the experiment (see Table 2). The experimental site is Suzhou Industrial Park Boai School & Clinic, China. Suzhou Industrial Park Boai School & Clinic is a public welfare

Table 1. MARG data performances specifications

Unit	Gyroscope	Accelerometer	Magnetometer
Dimensions	3 axis	3 axis	3 axis
Dynamic range	±1000 deg/s	±18 g	±1900uT
Sensitivity (/LSB)	0.04 deg/s	0.833 mg	142.9uguass
Bandwidth (kHz)	330	330	25
Linearity (% of FS)	0.2	0.2	0.1

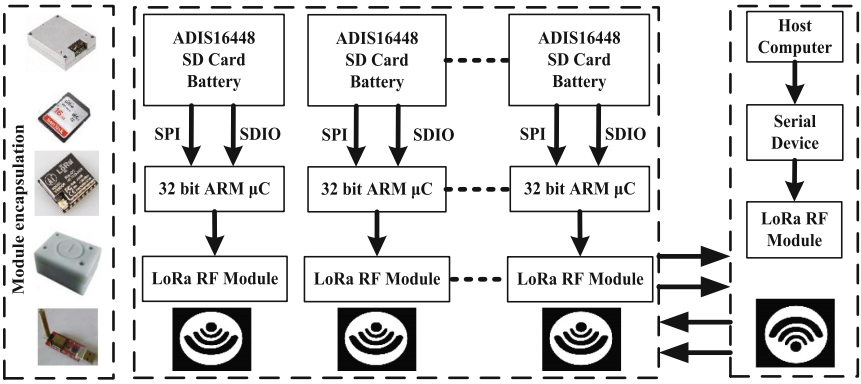

Fig. 1. The hardware of data acquisition system

school for disabled children donated by society, which has eight years experiences in hippotherapy. During the experiment, two therapists were also recruited to assist children and ensure safety.

Table 2. Participants' anthropometric details

Gender	Age (year)	Weight (kg)	Symptoms
Female	8	25.7	Hemiplegia with heel-toe, crouched gait
Female	10	29.6	Spastic diplegia of lower extremities
Male	12	30.2	Ataxia cerebral palsy, lower limb spasticity

During the experiment, ten inertial sensor nodes fitted on suitable nylon bandages were arranged on the surface of children' lumbar, chest, thigh, calf, upper arm and lower arm. Subsequently, the children ride on the horseback under the help of therapists, the groom leads the horse around a 30m×40m rectangular field and walks slowly. Therapists follow the horse on both sides to protect the children. After horse riding, all children will walk about 2 min in the designated corridor to collect gait data. Figure 2 shows the experimental scene.

Fig. 2. The experiment scene

3 Algorithm Structure

In this section, the proposed algorithm is described, which includes coordinate definition, signal pre-processing, orientation estimation algorithm, the method of motion capture, respectively.

3.1 Coordinate Definition

In our research, three coordinate systems were defined as follows:

(1) Navigation coordinate system (NCS): In this research, NCS is defined as the North-East-Down coordinate system (see Fig. 3). In summary, the X axis points to the North, the Y axis is perpendicular to the equator and points to the East, and Z axis is perpendicular to the ground and points to the center of the earth, respectively.
(2) Sensor coordinate system (SCS): The sensor frame is defined as the axes of SCS in Fig. 3.
(3) Body coordinate system (BCS): In this paper, every segment has its own coordinate system and specific definition refers to Fig. 3.

3.2 Signal Pre-processing

In the processing of sensor data, white noise interference often exists in the raw sensor data. Therefore, signal pre-processing is essential to reduce the sensor error caused by white noise. In our research, the process of signal pre-processing can be summarized as follows:

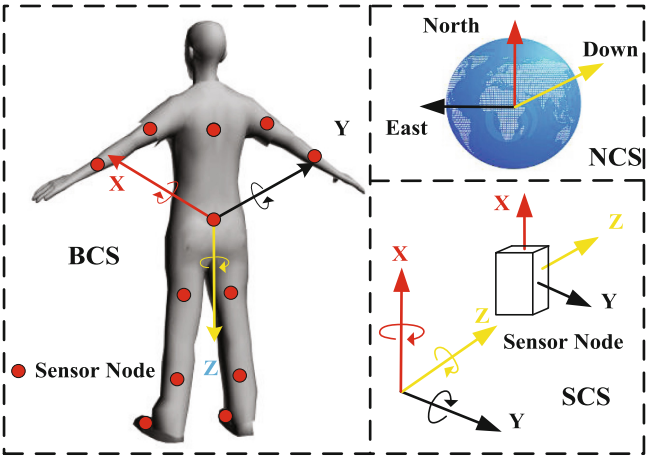

Fig. 3. The definition of coordinate system

Accelerometer: By analyzing the output of the accelerometer, it can be found that the outputs of the accelerometer contain more high-frequency components and the data oscillation is very serious. In order to filter the high-frequency part of the signal, a low-pass filter is used to filter the outputs of accelerometer.

Gyroscope: The error of the gyroscope is mainly on the zero drift, which can be simplified as the fluctuation of the output signal of gyroscope around the zero point in static state. In this paper, the weighted average filtering method is used to estimate the zero drift of gyroscope, so as to remove the influence of zero drift on the subsequent attitude calculation as much as possible.

Magnetometer: For magnetometer, it is mainly disturbed by the magnetic field of the surrounding environment, generally divided into soft iron interference and hard iron interference. In order to remove the local magnetic field interference, many studies have put forward relevant schemes [14] [15], among which an ellipsoid fitting method based on least squares [15] is effective. This method is also adopted by us to calibrate the magnetic field interference in this paper. Figure 4 shows the outputs of magnetometer before and after fitting. It can be found that before ellipsoid fitting, the outputs of magnetometer are approximately an ellipsoid and the center deviates from the origin, while the outputs of magnetometer are approximately a positive sphere after ellipsoid fitting.

3.3 Orientation Estimation Algorithm

In this research, our aim is to analysis the motor coordination function of children with CP. Motion coordination can be assessed by capturing children's movements. So orientation estimation algorithm should be used to measure the movements of children. In previous studies, there have been many related studies in such field, such as gradient descent algorithm [16], Kalman filter [17], complementary filter [18]. The main idea is to compute the estimation of orientation

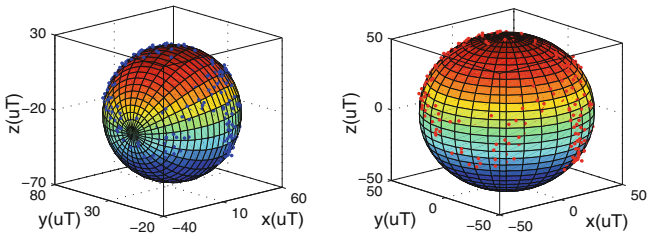

Fig. 4. The performance of ellipsoid fitting

through the optimal fusion of gyroscope, accelerometer, and magnetometer. In this paper, the gradient descent algorithm which is developed by Madgwick [16] is adopted for sensor fusion. In addition, on the basis of the original algorithm, the initial attitude calibration process is added to obtain more accurate results, and the process of algorithm is as follows.

(1) Initial Attitude Calibration

At first, considering the gimbal lock problem of euler angle and computational complexity of rotation matrix, quaternion representation is deployed in this research to describe the 3-D orientations of each limb. In general, a unit quaternion q can be expressed as

$$q = [q_0 \ q_1 \ q_2 \ q_3]^T \in H \tag{1}$$

where, $q_0 \in R$ and $[q_1 \ q_2 \ q_3]^T \in H$ are the scalar and the vector part of unit quaternion, respectively.

In order to express the movement of limbs in NCS, a series of attitude calibration should be conducted to make sure that the positions of sensors and limbs are fixed, which can guarantee the rotation quaternion between the sensor and corresponding body part is a fixed value. In our research, the calibration process is as follows: the subject is required to face the north and stand at up-right posture for a few seconds after he/she has worn the sensor nodes. In this way, the body frame BCS can be roughly overlapped with NCS. The initial alignment $q^N_{S,in}$ between SCS and NCS can be obtained by means of magnetometer and accelerometer as follows:

$$\phi_{in} = \arctan(a^y_s, a^z_s) \tag{2}$$

$$\theta_{in} = \arcsin(-a^x_s/g) \tag{3}$$

$$h^x_N = h^x_s \cos\theta_{in} + h^y_s \sin\theta_{in} \sin\phi_{in} + h^z_s \sin\theta_{in} \cos\phi_{in} \tag{4}$$

$$h^y_N = h^y_s \cos\phi_{in} - h^z_s \sin\phi_{in} \tag{5}$$

$$\varphi_{in} = -\arctan(h^y_N/h^x_N) \tag{6}$$

where, ϕ_{in}, θ_{in}, φ_{in} represent the roll, pitch and yaw, respectively; g indicates the acceleration of gravity, a^x_s,a^y_s,a^z_s and h^x_s, h^y_s, h^z_s represent three-axis acceleration

and three-axis magnetic field after calibration, respectively. Then, the initial quaternion q_S^N can be calculated from Eq. (7) through the mutual transformation between quaternion and Euler angles.

$$q_S^N = \begin{bmatrix} c(\phi_{in}/2)c(\theta_{in}/2)c(\varphi_{in}/2) + s(\phi_{in}/2)s(\theta_{in}/2)s(\varphi_{in}/2) \\ s(\phi_{in}/2)c(\theta_{in}/2)c(\varphi_{in}/2) - c(\phi_{in}/2)s(\theta_{in}/2)s(\varphi_{in}/2) \\ c(\phi_{in}/2)s(\theta_{in}/2)c(\varphi_{in}/2) + s(\phi_{in}/2)c(\theta_{in}/2)s(\varphi_{in}/2) \\ c(\phi_{in}/2)c(\theta_{in}/2)s(\varphi_{in}/2) - s(\phi_{in}/2)s(\theta_{in}/2)c(\varphi_{in}/2) \end{bmatrix} \quad (7)$$

where c and s represent cos and sin functions, respectively. As the coordinate frame of each body segment is aligned with NCS during the initialization, resulting in $q_S^B = q_S^N$. Of course, it must be declared that the few seconds of initial sensor-to-segment calibration is suitable for the case where the surrounding magnetic field interference remains unchanged and that this static standing calibration happens at a certain location for a very short time.

(2) orientation update

In this paper, the gradient descent algorithm which is developed by Madgwick [16] is adopted for sensor fusion. The gradient descent algorithm is introduced in document. At here, we will make a briefly description. The core idea is to approximate the minimum deviation model by continuous recursive iteration. The objective function can be defined as Eq. (8).

$$f(q_S^N, d^N, s^S) = (q_S^N)^* \otimes d^N \otimes q_S^N - s^S \to 0 \quad (8)$$

where q_S^N donates an orientation of the sensor, d^N represents a predefined reference direction of the field in the earth frame, s^S is the measured direction of the field in the sensor frame. The fusion process can be represented as Eq. (9) where λ_t and $(1 - \lambda_t)$ are weights applied to each orientation calculation.

$$q_{S,t}^N = \lambda_t q_{S,\nabla,t}^N + (1 - \lambda_t) q_{S,\omega,t}^N \qquad 0 < \lambda_t < 1 \quad (9)$$

3.4 The Method of Motion Capture

According to the principle of human kinematics, a human dynamic model based on skeletal vector is constructed, as shown in Fig. 5. The feature of this model is that each skeleton is connected by joints and traversed from top to bottom with pelvis as root point, so that the human posture can be obtained by combining the vectors of each body segment.

The vectors of each skeletal segment are defined in Fig. 5. O_B represents zero point. The position of the pelvis can be represented by the skeletal vectors in Eq. (10).

$$d_{\eta,\gamma}^B = \varsigma_{\eta,\gamma} \delta_{\eta,\gamma} \in R^3 \quad (10)$$

where η and γ denote the label of segments and limbs respectively. $d_{\eta,\gamma}^B$ is the vector of a body segment represented in BCS. $\varsigma_{\eta,\gamma} \in R$ is the length of a body

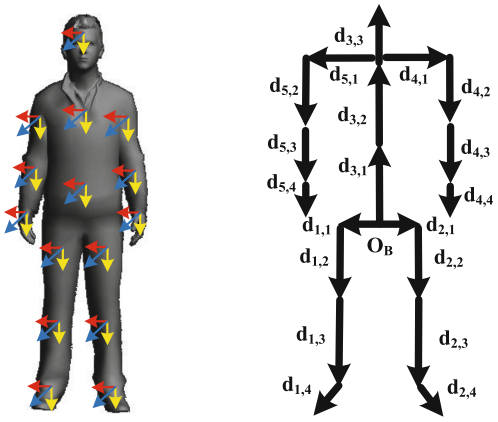

Fig. 5. The performance of ellipsoid fitting

segment. $\delta_{\eta,\gamma} \in R$ is the unit vector of a body segment in BCS. Through the initial attitude estimation, we can get q_S^B, After attitude updating, $q_S^N(t)$ can be measured. Thus the human body's posture in NCS can be expressed by Eq. (11).

$$q_B^N(t) = q_S^N(t) \otimes (q_S^B)^* \tag{11}$$

Then the posture of each limb vector under NCS can be expressed by Eq. (12).

$$d_{\eta,\gamma}^N(t) = q_{B,\eta,\gamma}^N(t) d_{\eta,\gamma}^B \tag{12}$$

where $d_{\eta,\gamma}^N(t)$ represents a vector of a body segment represented in NCS at time t. $q_{B,\eta,\gamma}^N(t)$ denotes the rotation quaternion of the corresponding skeletal segments converted from BCS to NCS at time t. At this moment, the position of each limb segment under NCS can be expressed by Eq. (13).

$$S_{\eta,\gamma}^N(t) = \sum_{t=0}^{n} d_{\eta,\gamma}^N(t) + O_N(t) \tag{13}$$

where $S_{\eta,\gamma}^N(t)$ is the position of joint between η, γ th and $\eta + 1$, γ th body segments, $O_N(t) \in R$ is the position of the center of pelvis at time t in NCS.

4 Experimental Results and Algorithm Validation

In this section, the accuracy of our method and experiment will be conducted. Firstly, Vicon optical system will be used for evaluating the accuracy of our method. Secondly, the motor posture of children with CP during hippotherapy will be captured to assess their motor coordination ability.

Fig. 6. The experimental scene of algorithm validation

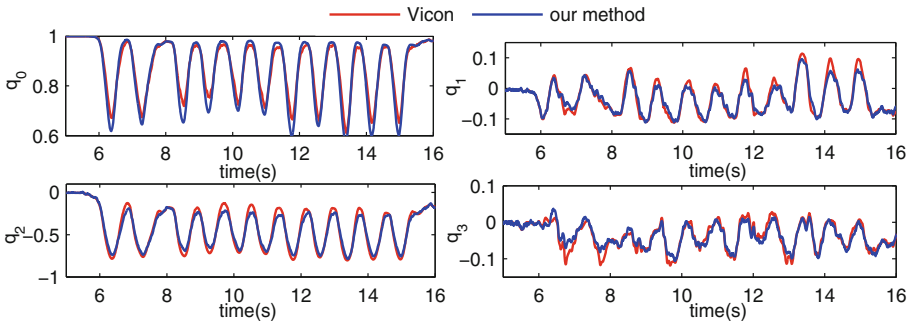

Fig. 7. The comparison of quaternion

4.1 Algorithm Validation

In this subsection, we use Vicon optical motion tracking system as a reference standard to verify the accuracy of the proposed algorithm. Vicon system is a well-known optical motion tracking system in the world, and its accuracy can reach 0.01 mm [19]. In this study, one participant participated in the measurement of the experiment. During the experiment, sensor nodes were arranged on the surface of the subject, and optical markers are arranged on the corresponding parts of the body. The experimental scene is shown in Fig. 6. The comparison of quaternion are shown in Fig. 7. It can be seen that the proposed method can track

Table 3. Estimation attitude comparison between our method and vicon

Angle	RMS(SD ± MEAN)(deg)	Correlation Coefficient
Yaw	1.2493(0.7313 + 0.5180)	0.9457
Pitch	0.2934(0.2183 + 0.0751)	0.9732
Roll	0.8249(0.4834 + 0.3415)	0.9581

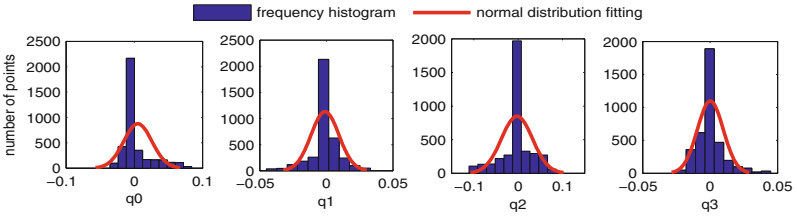

Fig. 8. Error statistics of quaternion

Vicon system accurately. Furthermore, the frequency histogram and normal distribution of quaternion are given in Fig. 8. It can be seen that the corresponding error mean and standard deviation of q0, q1, q2 and q3 are 0.0052, 0.0011, 0.0026, 0.0016 and 0.0116, 0.0105, 0.0141 and 0.0096, respectively. Table.3 lists the root-mean-square errors (RMSE) and correlation coefficients of the corresponding Euler angles. It can be seen that the corresponding RMSE are 1.2493, 0.2934 and 0.8249, the correlation coefficients are 0.9457, 0.9732 and 0.9581, respectively. The results show that our method is effective and estimation errors are well controlled.

4.2 Evaluation of Motion Coordination Ability

During the experiment, the inertial sensor nodes were arranged on the surface the pelvis, chest, upper arm, lower arm, thigh shank and feet of the children. With the help of the therapist, the children sat on the horseback and walked slowly. The children could adjust their posture by feeling the rhythm of the horse in the course of walking, so as to achieve the effect of improving muscle control. In this paper, we mainly measure the motor ability of children with cerebral palsy in the early stage of hippotherapy. In the experiment, in order describe the results clearly, a healthy child was introduced as a control group.

Figure 9 shows the raw sensor data of one child with CP in hippotherapy. Figure 10 shows the comparison of riding posture between CP and healthy children during hippotherapy. From Fig. 10, we can see that children with CP shows poor coordination with horses, posture distortion and can not control the balance of their limbs well at the early stage of treatment because of poor muscle tension and weak coordination ability. Figure 11 shows the contrast of joint angle between CP and healthy children. In Fig. 11, we mainly list the hip abduction/adduction and hip flexion/extension. We can see that in horse riding, children with cerebral palsy can not control their posture well because of their weak muscular tension, so their posture changes greatly during riding. Taking the hip flexion/extension for example, we can see the degree of flexion/extension of trunk corresponding to CP is usually large than healthy child. This indicates that children with CP have weak control over trunk balance, and muscle tone of waist is poor.

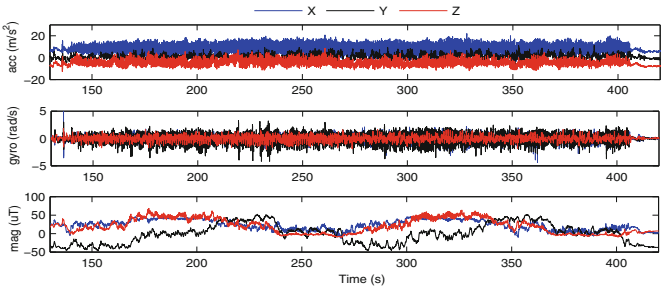

Fig. 9. The raw sensor data of one child with CP in hippotherapy.

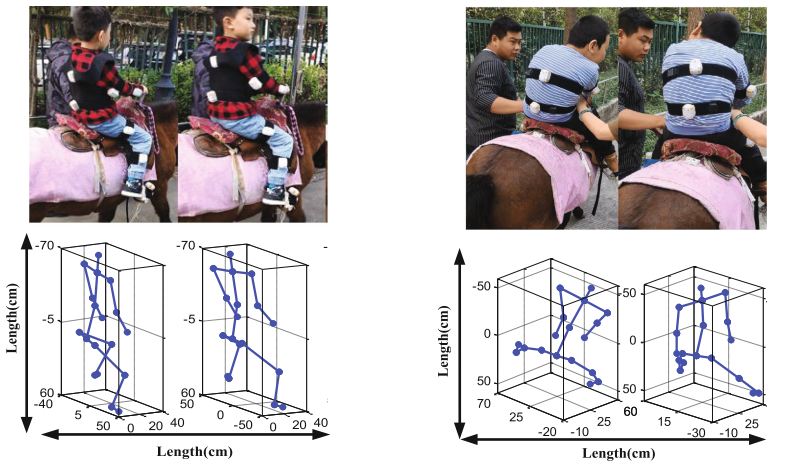

(a) The motion capture of healthy child (b) The motion capture of CP

Fig. 10. The comparison of motion capture between healthy and CP

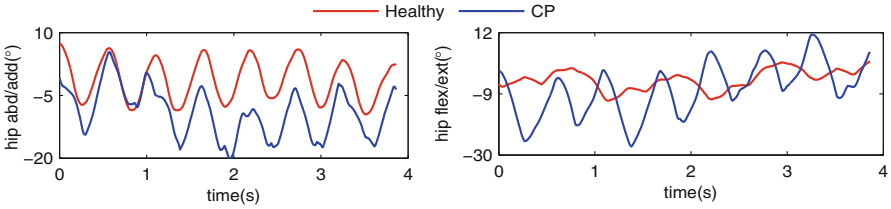

Fig. 11. Contrast of joint angle between healthy children and CP children.

In addition to the analysis of riding postures, we also analyzed the walking postures of CP and healthy children (see Fig. 12). Figure 12 shows that our method can effectively capture the child's movement posture. Through the comparison of CP and healthy children, it can be found that children with CP shows abnormally distorted when walking. In addition, we also counted the changes of

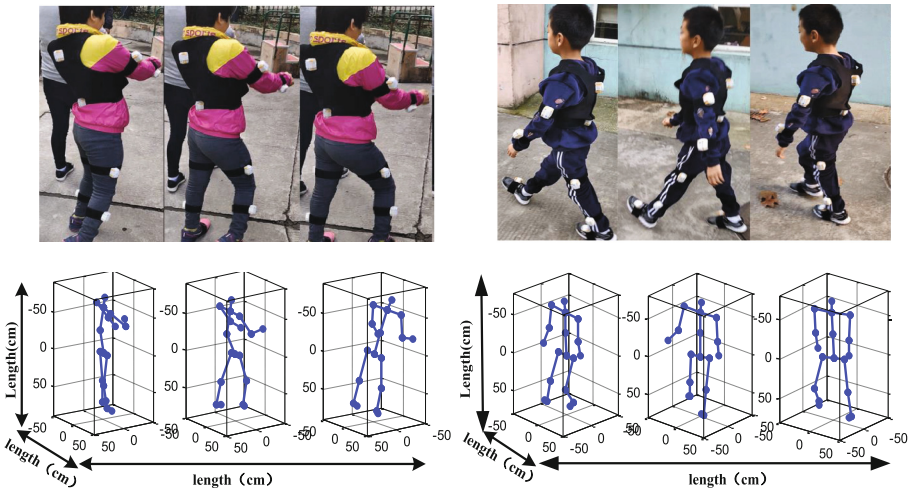

(a) The motion capture of healthy child (b) The motion capture of CP

Fig. 12. The comparison of motion capture between healthy and CP

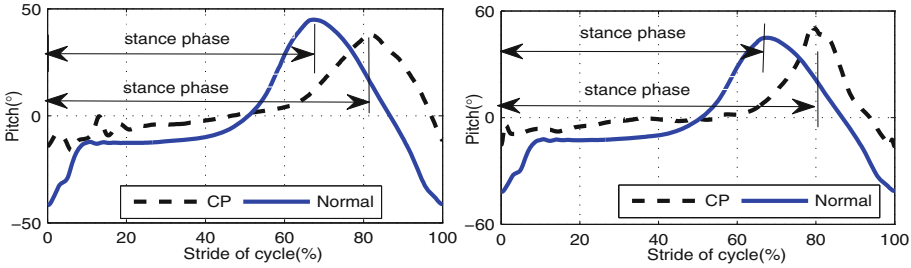

Fig. 13. Contrast of joint angle between healthy children and CP children.

the angle between foot plane and ground plane in the sagittal plane (equal to the pitch angle of foot) between CP and healthy children in walking. From Fig. 13, It can be found that the toe flexion is obvious and the dorsiflexion is very small in children with CP when walking normally. In addition, Fig. 13 shows that the proportions of stance phase of healthy children is about 65%, which is basically consistent with 60% of the actual measurements, while the children with CP maintained at about 80%, which indicates that the lower limbs of children with CP have motor deficits-crouch gait.

5 Conclusion

This paper introduces a method of motor measurement and evaluation for children with CP based on body area sensor network. The method uses wearable inertial sensors to measure the motor function of children with CP by sensor

fusion algorithm, whose accuracy is verified by optical system. In addition, via introducing the control group, the differences of motor coordination ability and gait parameters between children with CP and healthy children were discussed. Generally speaking, our method can effectively measure the movement posture and gait parameters of children with CP during hippotherapy, which provides a basis for proving the effectiveness of hippotherapy.

Acknowledgment. we would like to express our sincere thanks to Dalian Qiyu Ipony Equestrian Club Co. Ltd and Suzhou Industrial Park Boai School & Clinic for their support of this study.

References

1. Leung, B., Chau, T.: Single-trial analysis of inter-beat interval perturbations accompanying single-switch scanning: case series of three children with severe spastic quadriplegic cerebral palsy. IEEE Trans. Neural Syst. Rehabil. Eng. **24**(2), 261–271 (2016)
2. Hegde, N., et al.: The pediatric SmartShoe: wearable sensor system for ambulatory monitoring of physical activity and gait. IEEE Trans. Neural Syst. Rehabil. Eng. **26**(2), 477–486 (2018)
3. Stanley, J., Peake, J., Buchheit, M.: The effect of hydrotherapy on cardiac parasympathetic recovery and exercise performance. J. Sci. Med. Sport **13**(supp–S1), 51–52 (2010)
4. Field, T., Largie, S., Diego, M., Manigat, N., Seoanes, J., Bornstein, J.: Cerebral palsy symptoms in children decreased following massage therapy. Early Child Dev. Care **175**(5), 445–456 (2005)
5. Naimo, P.S., et al.: Surgical intervention for anomalous origin of left coronary artery from the pulmonary artery in children: a long-term follow-up. Ann. Thorac. Surg. **101**(5), 1842–1848 (2016)
6. Wang, Z., et al.: Inertial sensor-based analysis of equestrian sports between beginner and professional riders under different horse gaits. IEEE Trans. Instrum. Meas. **67**(11), 2692–2704 (2018)
7. Debuse, D., Gibb, C., Chandler, C.: Effects of hippotherapy on people with cerebral palsy from the users perspective: a qualitative study. Physiotherapy Theory Pract. **25**(3), 174–192 (2009)
8. Lee, C.-W., Gil, K.S., Sik, Y.M.: Effects of hippotherapy on recovery of gait and balance ability in patients with stroke. J. Phys. Therapy Sci. **26**(2), 309–311 (2014)
9. Lee, N., Park, S., Kim, J.: Effects of hippotherapy on brain function, BDNF level, and physical fitness in children with ADHD. J. Exerc. Nutr. Biochem. **19**(2), 115–121 (2015)
10. Park, E.S., Rha, D.-W., Shin, J.S., Kim, S., Jung, S.: Effects of hippotherapy on gross motor function and functional performance of children with cerebral palsy. Yonsei Med. J. **55**(6), 1736–1742 (2014)
11. Wang, Z., Zhao, H., Qiu, S., Gao, Q.: Stance-phase detection for ZUPT-aided foot-mounted pedestrian navigation system. IEEE/ASME Trans. Mechatron. **20**(6), 3170–3181 (2015)
12. Qiu, S., Wang, Z., Zhao, H., Huosheng, H.: Using distributed wearable sensors to measure and evaluate human lower limb motions. IEEE Trans. Instrum. Meas. **65**(4), 939–950 (2016)

13. Yuan, Q., Chen, I.-M.: Human velocity and dynamic behavior tracking method for inertial capture system. Sens. Actuators **183**, 123–131 (2012)
14. Vicente, A.O., Garcia, G.R., Olivares, G., Górriz, J.M., Ramirez, J.: Automatic determination of validity of input data used in ellipsoid fitting MARG calibration algorithms. Sensors **13**(9), 797–817 (2013)
15. Kok, M., Schön, T.B.: Magnetometer calibration using inertial sensors. IEEE Sens. J. **16**(4), 5679–5689 (2016)
16. Madgwick, S.O.H., Harrison, A.J.L., Vaidyanathan, R.: Estimation of IMU and MARG orientation using a gradient descent algorithm. In: IEEE International Conference on Rehabilitation Robotics, pp. 1–7. IEEE, Switzerland (2011)
17. Zhang, Z., Meng, X., Wu, J.: Quaternion-based Kalman filter with vector selection for accurate orientation tracking. IEEE Trans. Instrum. Meas. **61**(10), 2817–2824 (2012)
18. Mahony, R., Hamel, T., Pflimlin, J.M.: Nonlinear complementary filters on the special orthogonal group. IEEE Trans. Autom. Control **53**(5), 1203–1218 (2008)
19. Oxford Metrics, Vicon Motion Systems (2019). https://www.vicon.com